16. MINERALOGY AND GEOCHEMISTRY OF WEATHERED SERPENTINITES, DEEP SEA DRILLING PROJECT LEG 84[1]

Roger Helm, Geologisches Institut, Ruhr-Universität[2]

ABSTRACT

At Sites 566, 567, and 570 of Leg 84, ophiolitic serpentinite basement was covered by a sequence of serpentinitic mud that was formed by weathering of the serpentinites under sea- or pore-water conditions. Several mineralogical processes were observed: (1) The serpentinitic mud that consists mainly of chrysotile was formed from the lizardite component of the serpentinites by alteration. (2) Slightly trioctahedral smectites containing nonexpandable mica layers, trioctahedral smectites containing nonexpandable chlorite layers, and swelling chlorites were presumably formed from detrital chlorite and/or serpentine. (3) The occurrence of tremolite, chlorite, analcime, and talc can be attributed to reworking of gabbroic ophiolite rocks. (4) Dolomite, aragonite, and Mg-calcite, all authigenic, occur in the serpentinitic mud.

INTRODUCTION

Serpentinitic muds were recovered above serpentinitic basement rocks at Sites 566, 567, and 570. At all sites where ultramafic ophiolitic rocks were recovered, serpentinitic muds with or without calcareous admixtures were recovered above the serpentinites. The muds are interpreted to be the result of submarine weathering of the underlying serpentinites. The mineralogy and chemistry of these serpentinitic muds are discussed in this chapter.

Methods

The sediment was dispersed using a high-frequency stirrer in deionized water. The fractions >63 μm and <63 μm were separated by sieving. These samples were studied using X-ray diffraction (Cu, Kα), infrared spectroscopy, and differential thermal analyses (DTA). The chemical analyses were carried out by X-ray fluorescence using the $Li_2B_4O_7/LiBO_2$ glass disk method. An electron microscope with an additional energy dispersive spectrometer (EDAX) was used to identify the morphology of the minerals.

LITHOLOGY

In Hole 566 (Fig. 1) the serpentinites are covered by a serpentinitic mud sequence with aragonite and dolomite admixtures. Aragonite is found as fibrous concretions, and dolomicrite occurs containing dispersed serpentinite clasts. The muds have a thickness of about 2 m and pass directly into the serpentinites. Aragonite- and dolomite-filled joints occur in the basement rocks. The serpentinitic muds are covered by typical hemipelagic slope sediments of the late Pleistocene.

In Hole 566C (Fig. 1) pure serpentinitic mud (~ 3 m) covers the hard rocks. The transition between mud and serpentinites shows a continuous increase of solid serpentine fragments in the muddy matrix with depth. Late Miocene slope sediments cover the serpentinitic muds without a mixing zone.

At Site 567 (Fig. 1) serpentinitic muds about 1 m thick were first recovered in Core 7. Angular clasts of dark green unweathered serpentinite are dispersed in the muddy groundmass. The serpentinitic mud shows colors from dusky blue to grayish blue. Dolomite was found in the serpentinitic mud. This serpentinite occurrence within early Miocene slope sediments was probably a boulder transported from upslope by slumping, and little evidence for mixing between serpentinitic mud and typical slope sediment was observed by the shipboard scientists (Site 567 report, this volume). A second occurrence of serpentinitic mud and serpentinites was recovered beneath the first at a sub-bottom depth of 320 to 350 m. Black and dark greenish serpentinite clasts are dispersed in a pale blue to grayish blue or pale green serpentinitic mud. The upper contact is developed as a transition zone between slope sediment and serpentinitic mud (567-14-2, 40–80 cm). The nature of the contact between serpentinites and the underlying Miocene mud is unclear. The Miocene mud may be a downhole contaminant. In this case, the ultramafic material belongs to an ophiolitic assemblage that was drilled in the basal section at Site 567. The assemblage contains deep-water Cretaceous limestone, basalts, dolerites, gabbros, and ultramafics. This section contains all the components of an ophiolite complex (Coleman, 1977). The serpentinitic muds generally contain admixtures of gabbroic material. Alternatively, if the Miocene mud is in place, the serpentinitic mud was probably emplaced by slumping from upslope.

At Site 570 (Fig. 1) serpentinitic mud was recovered below completely consolidated early Eocene sediments (Core 39). About 10 m of serpentinitic mud with admixtures of serpentine clasts were drilled above the massive serpentinites. The color of these muds ranges from pale blue to green. The dark green serpentine clasts are veined by pale green to white fissures (hydrotalcite and chrysotile) (Fig. 2). Because the veins do not continue into the matrix, they must have been formed prior to the serpentinitic muds.

MINERALOGY

Electron microscope investigations show that the serpentinitic mud consists of silt-sized serpentine aggregates

[1] von Huene, R., Aubouin, J., et al., *Init. Repts. DSDP*, 84: Washington (U.S. Govt. Printing Office).

[2] Address: Geologisches Institut, Ruhr-Universität, Bochum, West Germany.

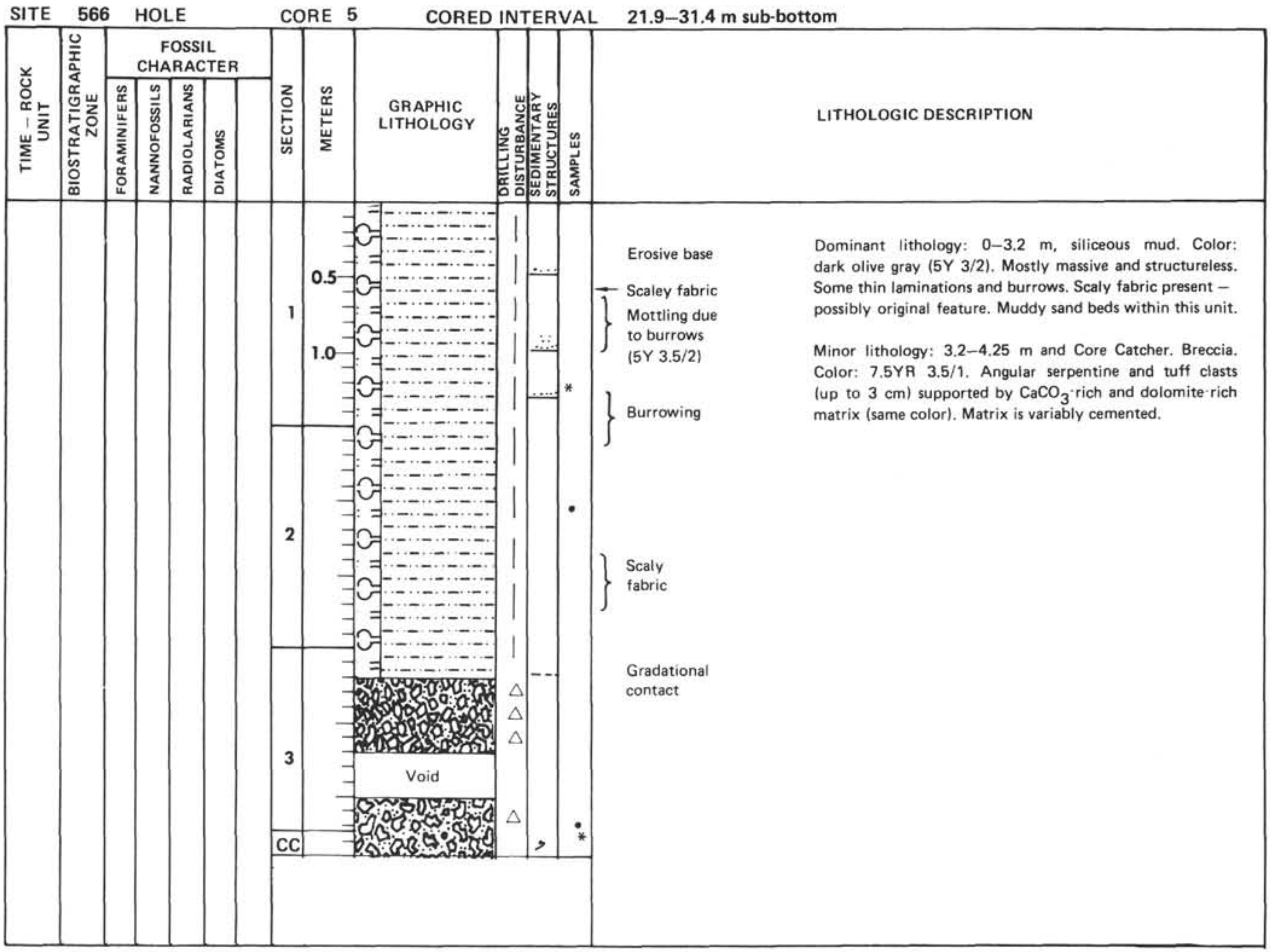

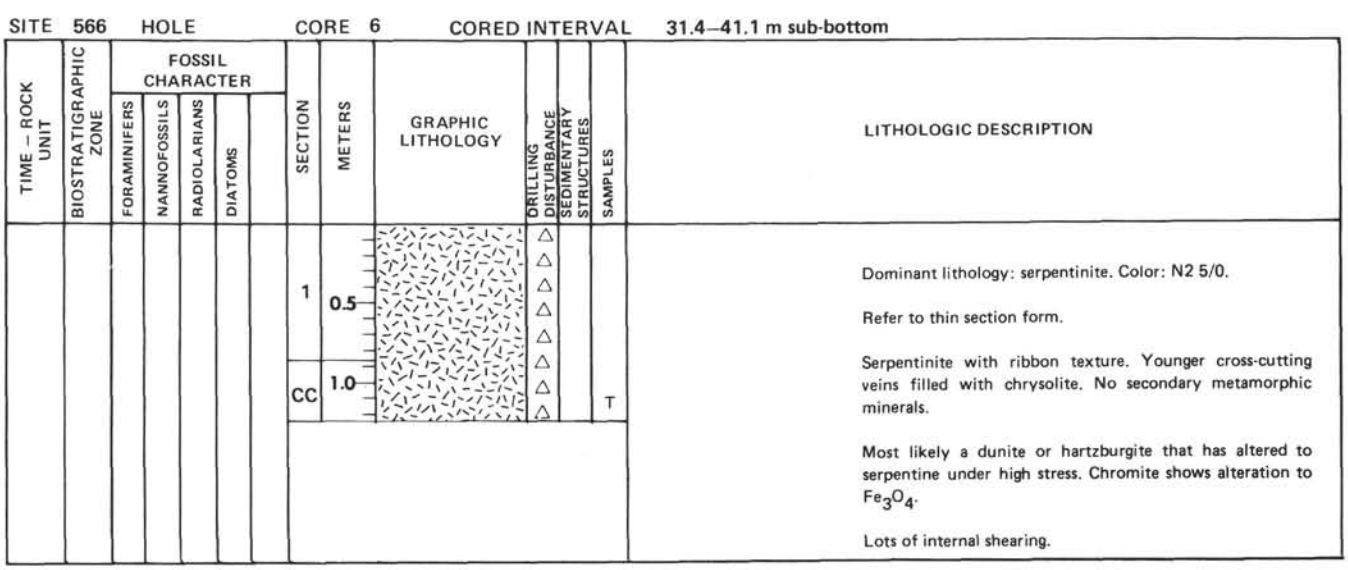

Figure 1. Lithology columns showing contact between average slope sediment and serpentinitic mud as well as contact between serpentinitic mud and massive serpentinite.

SITE 566 HOLE C CORE H2 CORED INTERVAL 88.1–109.1 m sub-bottom

TIME – ROCK UNIT	BIOSTRATIGRAPHIC ZONE	FOSSIL CHARACTER: FORAMINIFERS	NANNOFOSSILS	RADIOLARIANS	DIATOMS	SECTION	METERS	GRAPHIC LITHOLOGY	DRILLING DISTURBANCE	SEDIMENTARY STRUCTURES	SAMPLES	LITHOLOGIC DESCRIPTION
late Miocene						1	0.5 1.0	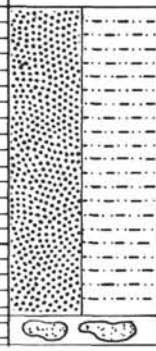	□ □ □		* *	Structureless drilling breccia comprising two dominant lithologies. Mudstone. Color: dark olive gray (5Y3 5/2). Structureless. Sandstone. Color: dark greenish gray (5GY 4/2). Lithified sandstone, matrix rich in $CaCO_3$. Sand- to gravel-sized grains. High percentage of volcanic rock fragments – angular. No internal sedimentary structures.
						2			□			
						CC					*	

SITE 566 HOLE C CORE 5 CORED INTERVAL 109.1–117.2 m sub-bottom

TIME – ROCK UNIT	BIOSTRATIGRAPHIC ZONE	FOSSIL CHARACTER: FORAMINIFERS	NANNOFOSSILS	RADIOLARIANS	DIATOMS	SECTION	METERS	GRAPHIC LITHOLOGY	DRILLING DISTURBANCE	SEDIMENTARY STRUCTURES	SAMPLES	LITHOLOGIC DESCRIPTION
						1	0.5 1.0	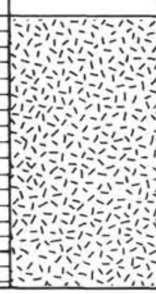	□ □ □ □			Dominant lithology: serpentinite and remnants of serpentinized peridotite. Color: dusky blue (5BP 3/2). See igneous rock core description. This core has been highly disturbed by drilling. The serpentinite has weathered to a clay – some original structures visible. Intact, unweathered blocks of peridotite found throughout the core.
						CC						

Figure 1. (Continued).

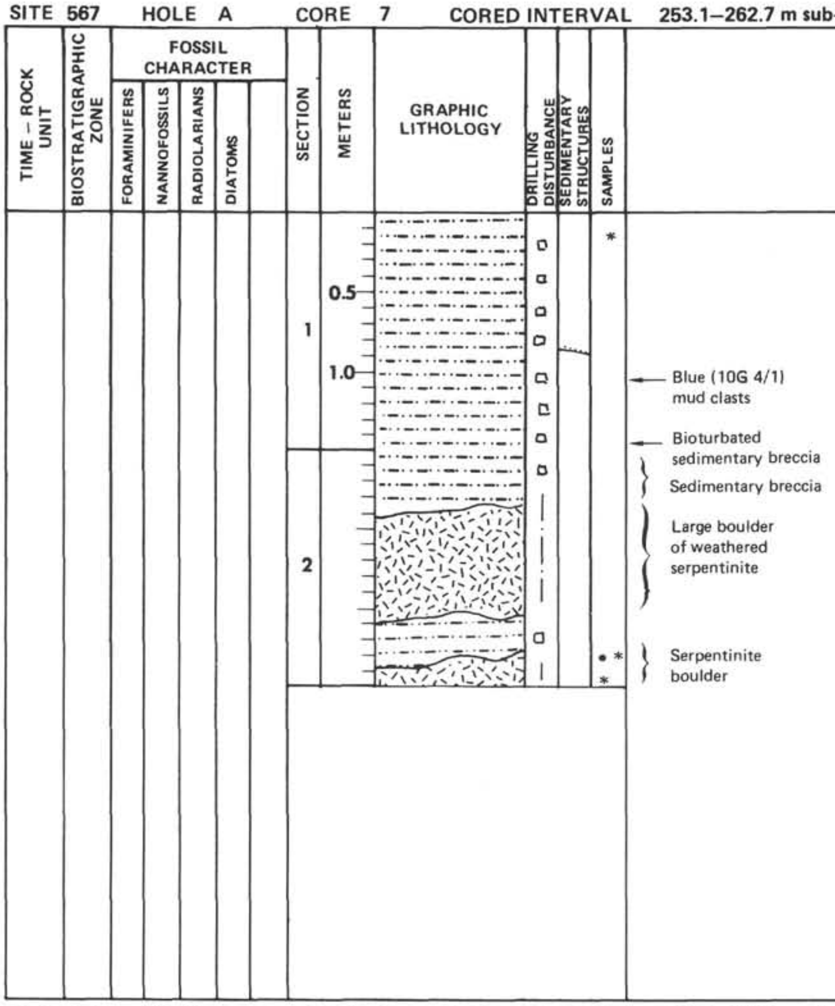

LITHOLOGIC DESCRIPTION

Dominant lithology: mudstone. Color: grayish olive green (5GY 3/2) to pale green (10G 6/2).

Structureless – dominated by sedimentary breccias with blue clast up to 2 cm in diameter. Matrix and clast supported. Dolomitic around serpentinite clasts.

Minor lithology: serpentinite. Color: dusky blue (5PB 3/2) to grayish blue (5PB 5/2). Present as large clasts within the mud. Original structures visible – truncated at margins of the boulder. Larger boulder may comprise smaller clasts.

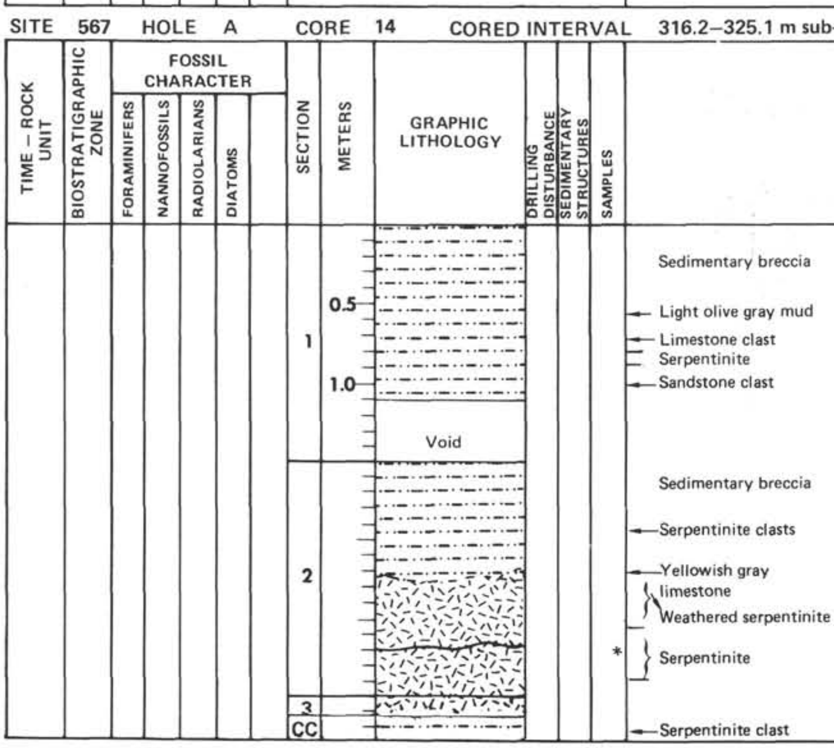

LITHOLOGIC DESCRIPTION

Dominant lithology: mud. Color: brownish black (5YR 2/1) to olive black (5Y 2/1). Massive mudstone – sedimentary breccia with assorted clasts.

Minor lithology: serpentinite. Color: very pale blue (5B 8/2) and black – unweathered.

Figure 1. (Continued).

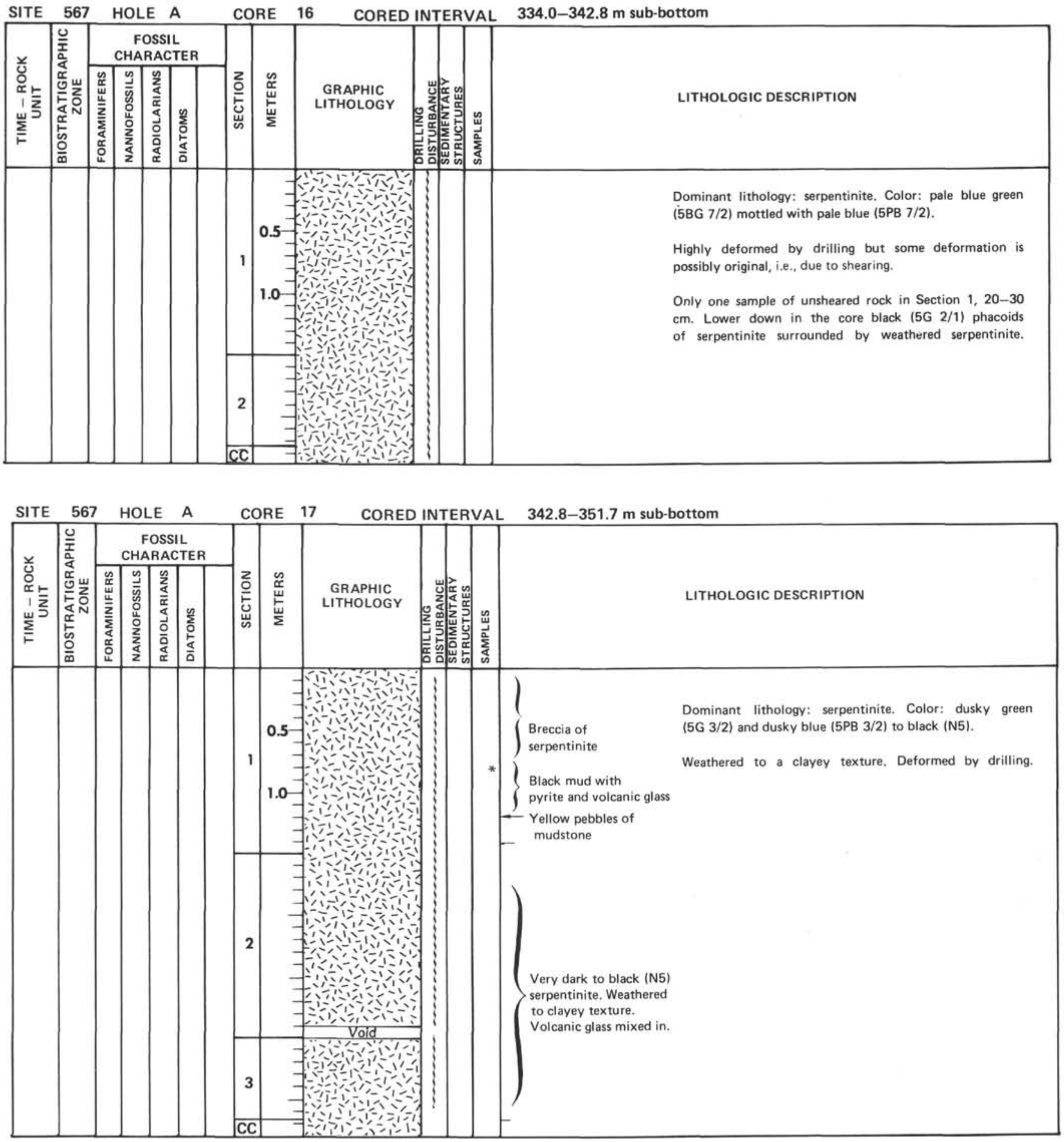

Figure 1. (Continued).

of 2- to 10-μm-long chrysotile fibers (Plate 1, Fig. 1). High-magnification electron photomicrographs show that the chrysotile aggregates consist of more or less isolated fibers (Plate 1, Fig. 3). On the other hand, the predominant serpentine mineral in the serpentinites is lizardite, as identified by X-ray diffraction. Electron photomicrographs show the platy morphology of this serpentine mineral: Plate 2, Fig. 2, showing a chrysotile vein in a massive serpentinite, demonstrates the different morphology of fibrous chrysotile and platy lizardite, whereas Plate 1, Fig. 2 exhibits an oblique section of lizardite plates. Aggregates that consist of fibrous chrysotile, but are still arranged like bundles (Plate 1, Fig. 4 and Plate 2, Fig. 4), may indicate that the chrysotile fibers were formed by splitting up of the platy lizardite sheets. This transformation is attributed to the different crystal structure of lizardite and chrysotile. The fibers of chrysotile consist of layers that are curled into cylindrical rolls,

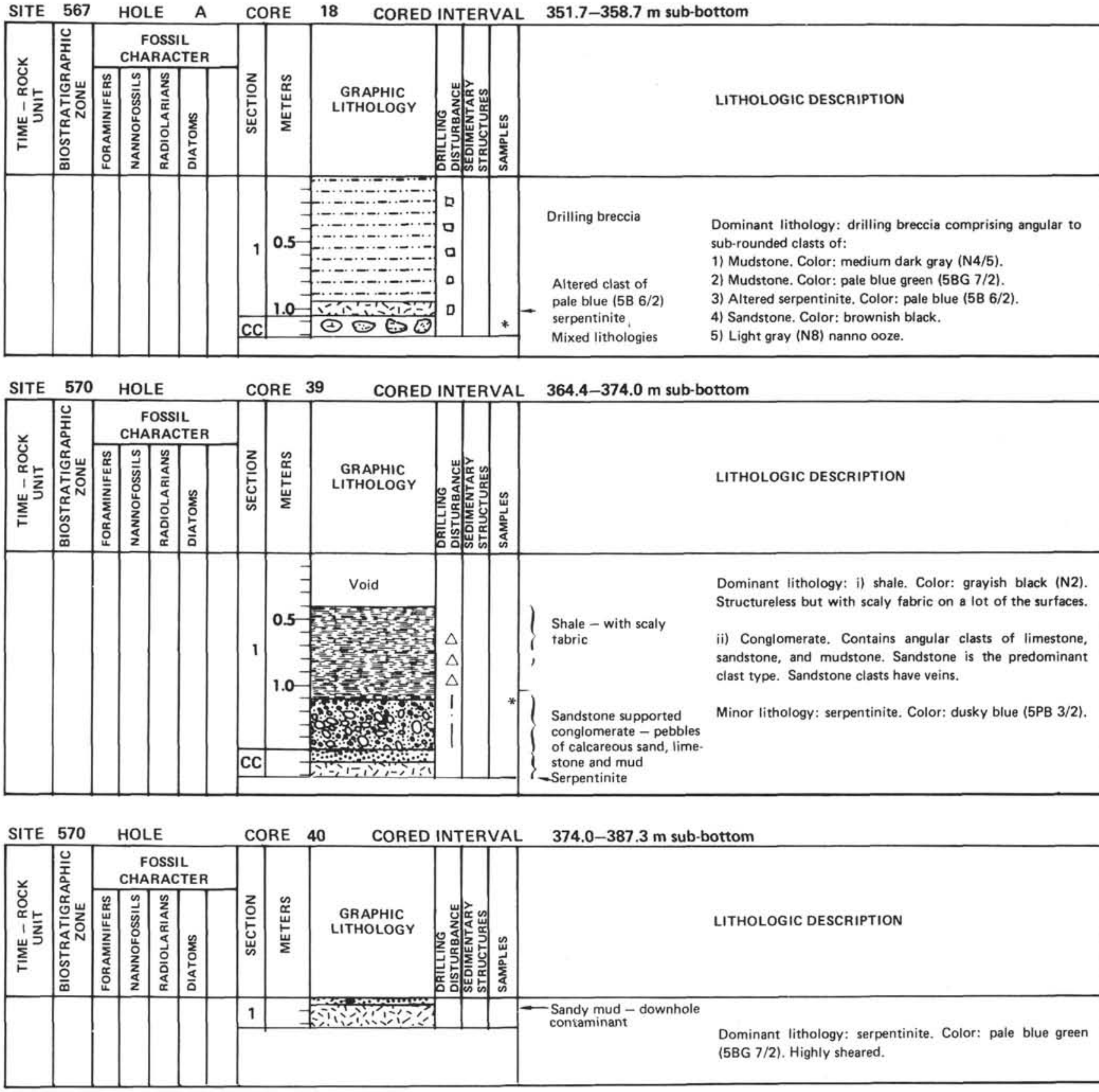

Figure 1. (Continued).

whereas the lizardite shows a planar crystal structure (Brindley and Brown, 1980). The conjecture that chrysotile fibers were formed by splitting up of lizardite plates is supported by a different appearance of fibrous chrysotile in veins of the solid serpentinites (Plate 2, Figs. 1 and 2), where the chrysotile presumably was precipitated from solution. It is very common in ultramafic rocks to have olivine and pyroxenes completely replaced by lizardite, with subsequent crystallization of chrysotile as vein fillings and the replacing of lizardite by chrysotile (Prichard, 1979). This distribution of chrysotile and lizardite in ultramafic rocks as reported in Prichard (1979) indicates that the chrysotile in the serpentinitic muds drilled off Guatemala was formed from the lizardite component of the serpentinites by weathering processes.

According to X-ray diffraction results, the serpentinites consist of lizardite, and the serpentinitic muds consist chiefly of chrysotile. The latter can be identified in the serpentinites only if pale green veins are abundant. Lizardite in the serpentinitic mud, especially in the >63 μm fraction, is the result of unweathered serpentinite clasts. The serpentine minerals were determined by criteria described in Mumpton and Thompson (1975). The X-ray diffraction investigations (Table 1) do not provide further information about the alteration process. All characteristic d-spacings of lizardite and chrysotile are de-

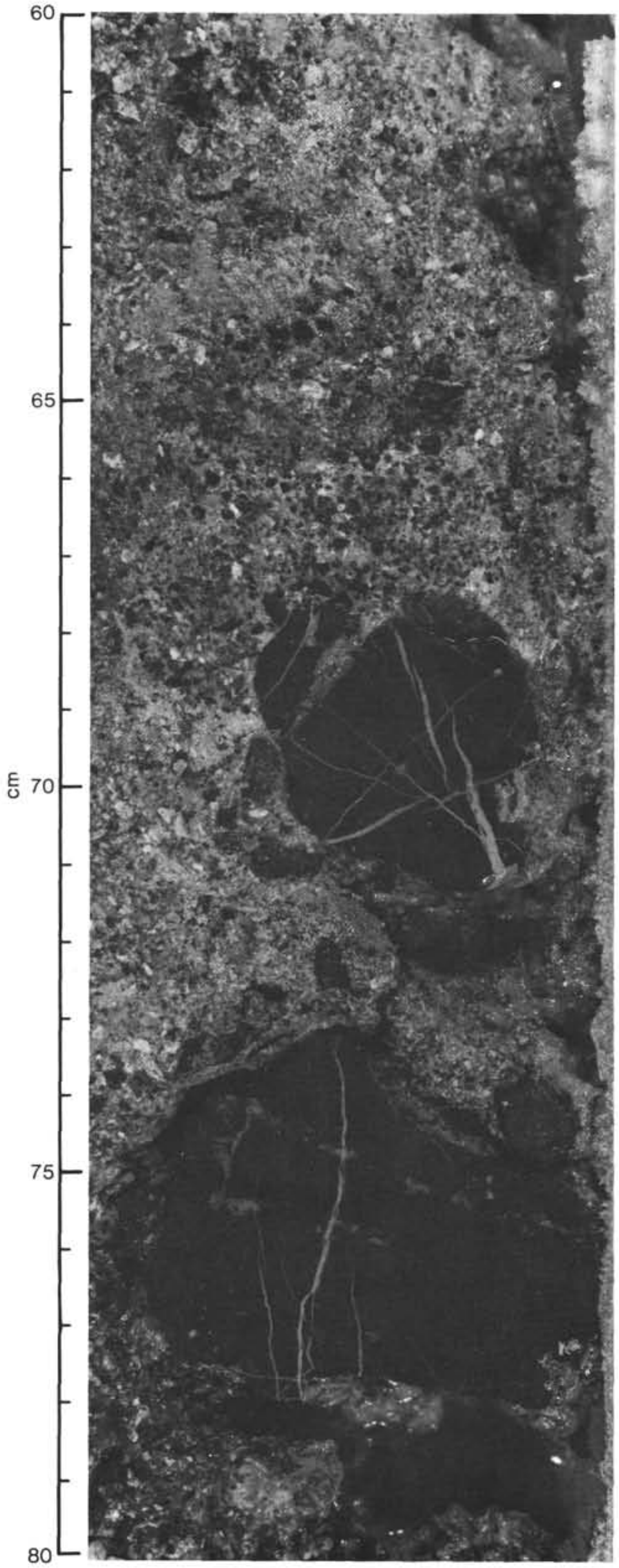

Figure 2. Example of serpentinitic mud section with clasts of veined serpentinite from Hole 570, Core 41, Section 2, 60–80 cm.

Table 1. Mineral composition of serpentinitic mud (>63 μm and <63 μm) and serpentinites.

Sample (interval in cm)	Serpentine mineral	Rock type	Grain size fraction (μm)
566C-5-1, 1–29	Lizardite	Serpentinite	—
566C-6-1, 82–84	Lizardite	Serpentinite	—
567-14-2, 134–135	Lizardite	Serpentinite	—
570-41,CC (10–13)	Lizardite	Serpentinite	—
567-7-2, 77–79	Lizardite–chrysotile	Serpentinite mud	>63
567-7-2, 77–79	Chrysotile–lizardite	Serpentinite mud	<63
567-17-3, 35–37	Chrysotile–lizardite	Serpentinite mud	<63
567-17-3, 35–37	Lizardite–chrysotile	Serpentinite mud	>63
570-39,CC (5–10)	Chrysotile	Serpentinite mud	>63
570-39,CC (5–10)	Chrysotile	Serpentinite mud	<63
570-40,CC (7–9)	Chrysotile–lizardite	Serpentinite mud	>63
570-40,CC (7–9)	Chrysotile	Serpentinite mud	<63
570-41-1, 78–80	Chrysotile–lizardite	Serpentinite mud	>63
570-41-1, 78–80	Chrysotile	Serpentinite mud	<63
570-41-4, 31–33	Chrysotile–lizardite	Serpentinite mud	>63
570-41-4, 31–33	Chrysotile	Serpentinite mud	<63

Note: — indicates that the first four samples are hard rock, so they have no grain size.

veloped at once: a transitional change of X-ray diffraction patterns cannot be determined. Infrared spectroscopy studies also demonstrate that the massive serpentinites consist of lizardite and that the serpentinitic muds consist of chrysotile (Fig. 3). The different bands in the spectra were attributed to chrysotile and lizardite by criteria described in Yariv and Heller-Kallai (1975).

The occurrence of the serpentine minerals of the chrysotile–lizardite group is supported by differential thermal analyses (DTA). Though Faust and Fahey (1962) stated that chrysotile cannot be distinguished from lizardite by DTA, the present samples show slightly different DTA curves for serpentinite and serpentinitic muds (Fig. 4). It is yet unclear whether these differences can be related to additional minerals that were not detected by X-ray diffraction and infrared spectroscopy or to weathering effects. According to Mackenzie (1957), there are distinct differences in the DTA curves of weathered versus unweathered samples of serpentinite containing the same minerals.

Chlorite, tremolite, talc, analcime, and swelling clay minerals have been determined in the serpentinitic muds at Sites 566 and 567 by X-ray diffraction and electron microscopy using an EDAX system. The swelling clay minerals occur either in serpentinitic muds that contain gabbroic material (567-21,CC [130–132 cm]) or in serpentinitic muds containing admixtures of the typical slope sediments (567-14-2, 131–133 cm). Tremolite, talc, chlorite, and analcime have been detected in the retrograde metamorphic gabbroic rocks drilled in the lower sections of Holes 567 and 569A (see site reports, this volume). These minerals are generally enriched in the >63-μm fraction of the serpentinitic muds and can be identified in gabbroic rock clasts under the electron microscope with an additional EDAX system (Plate 2, Fig. 3). So these minerals are presumably the result of a reworking of gabbroic rocks that occur together with the serpentinites at the drilled sites. Analcime was also found in the serpentinitic muds containing admixtures of slope sediment (567-14-2, 131-133 cm). In these sediments, analcime was pre-

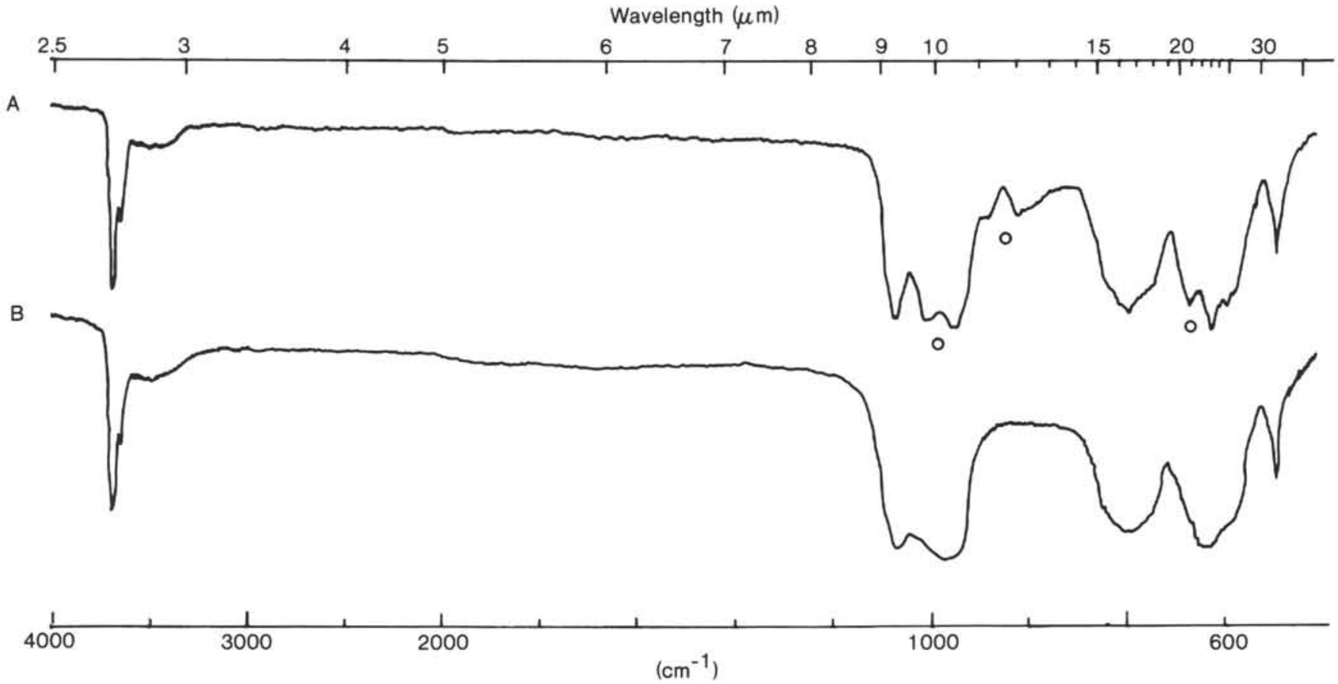

Figure 3. Infrared spectra of (A) chrysotile, Sample 570-4,CC (7–9 cm) <63 μm, and (B) lizardite, Sample 570-41,CC (10-13 cm). (Characteristic differences are indicated by an open circle.)

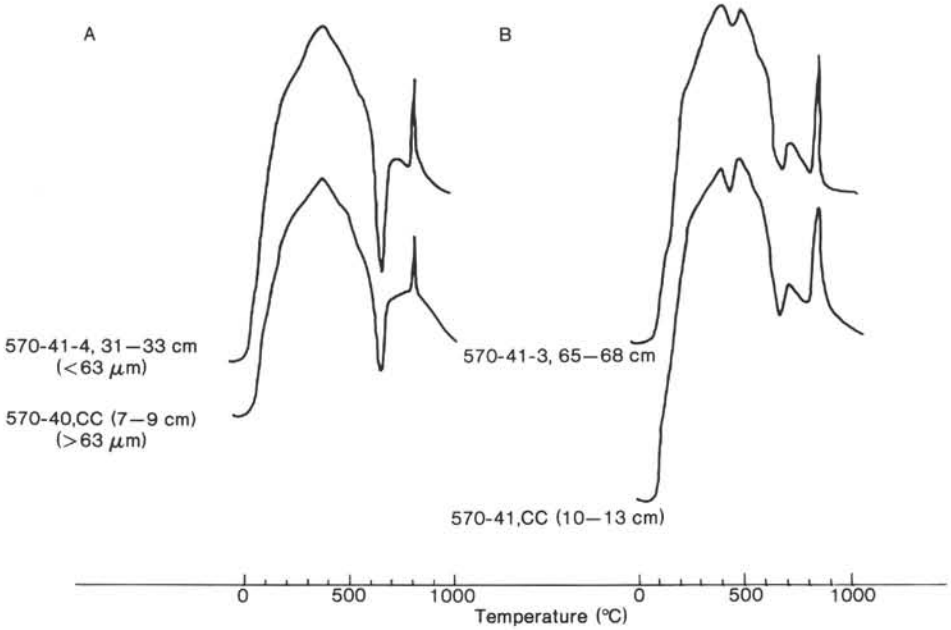

Figure 4. Differential thermal analyses curves for (A) serpentinitic mud (chrysotile) and (B) massive serpentinite (lizardite).

sumably formed from the slope sediment's clinoptilolite after a mixing with the serpentinitic mud. Because of an increase of the Na^+/H^+ ratio during serpentine weathering that causes an increase of pH (Barnes and O'Neil, 1969) clinoptilolite is replaced by analcime (Boles, 1971). The swelling clay minerals are strongly enriched in the <63-μm fraction of the serpentinitic muds and are believed to be alteration products of chlorite and/or serpentine. The main swelling clay mineral is a trioctahedral smectite (saponite?) containing nonexpandable chlorite layers. The (002)-spacing value of this mixed layer mineral can be attributed to 5 to 10% chlorite layers (Brindley and Brown, 1980). Additional swelling clay minerals are illite–montmorillonite (slightly trioctahedral) and swelling chlorite (Table 2). Swelling clay minerals that show 14-Å spacings untreated and 12.6 Å spacings

Table 2. Expandable clay minerals in serpentinitic muds.

	d-spacings (Å) of swelling clay minerals (Cu, Kα)							
	(001)				(002)	(003)	(060)	
Sample	Untreated	Glyc.	350°C	500°C	Glyc.	Glyc.	Nonoriented	Minerals
567-14-2, 131–133 cm (<2 μm)	14.9	16.8	14.5	14 + 10	8.47	5.58	1.531 1.506	Trioctahedral smectite with ~10% chlorite, di-trioctahedral smectite with about 15% illite
567-17-1, 110–112 cm (<2 μm)	14.8	16.7	10 + 14	14 + 10	8.43	5.61	1.531 1.507	Trioctahedral semctite with about 10% chlorite, di-trioctahedral smectite with about 5% illite
567-20-1, 17–20 cm (<2 μm)	12.5	16.7	10 + 14	14 + 10	8.43	5.59	1.535 1.51	Trioctahedral smectite with about 10% chlorite and slightly trioctahedral smectite containing about 10% illite layers
567-23-1, 20–21 cm (<63 μm)	14.9	17.0	14.9	14.4			1.52	Swelling chlorite
567-21,CC (4–6 cm) (<63 μm)	14.6	16.8	14.6	14.2			1.536	Swelling chlorite
567-29-2, 130–132 cm (<63 μm)	14.9	16.9	14.5	14 12.6			1.535 1.506	Mixed layer of the smectite–chlorite group, di-trioctahedral smectite
567-27-1, 80–82 cm (<63 μm)	14.8	16.7	10 + 14	14 10	8.46	5.59	1.53 1.506	Trioctahedral smectite with ~10% chlorite, di-trioctahedral smectite containing about 10% illite

Note: The first column refers to the (001) d-spacing of swelling clay minerals; 10 and 14 under 350°C and 14 and 10 under 500°C mean that two different d-spacings are developed after heating. The second column (002) refers to a d-spacing (glycol.) of a trioctahedral smectite-chlorite mixed mineral. The third (003) column refers to a d-spacing (glycol.) of a di-trioctahedral smectite–illite mixed layer mineral. The fourth column refers to (060) d-spacings of expandable clay minerals. If two peaks occur, they refer to a trioctahedral and a more dioctahedral clay mineral in the same sample.

after heating to 500°C may be also chlorite–montmorillonite mixed layers (Thorez, 1975) (see Fig.5).

Dolomite and aragonite have also been detected in the serpentinitic muds. Aragonite appears as fibrous concretions in serpentinitic muds and joint fillings in massive serpentinites. Dolomite was observed as joint fillings and dolomicrites (dolomite crystals ~10 μm) including serpentine clasts. The Sr/Ca mole ratios of the carbonates indicate that they were formed in equilibrium with sea- or shallow pore water rather than with deep pore water (see Helm, this volume). However, it is not clear whether the dolomite in the serpentinitic muds of Holes 566 and 566C was formed by direct precipitation or by replacement of aragonite or calcite.

The basic Mg-Al carbonate hydrotalcite (Mg_6Al_2 $[CO_3]$ $[OH]_{16} \times 4H_2O$) was identified using X-ray diffraction in serpentinites and serpentinitic muds Sites 566, 567, and 570. It occurs together with fibrous chrysotile in the veins of massive serpentinites. These hydrotalcite and chrysotile veins in the serpentinite clasts dispersed in the serpentinitic muds are cut off by the muddy groundmass. This indicates a formation of hydrotalcite prior to the formation of the serpentinitic muds, perhaps in a very low grade hydrothermal process.

GEOCHEMISTY

The geochemical and mineralogical properties of the serpentinitic muds separate this sediment into three different types:

1. *Pure serpentinitic mud.* Only slight differences (Sample 570-40,CC [5–10 cm]) of the chemical composition can be observed: In general, Zn, Cu, P, Rb, and sometimes Ba show a slight enrichment in this group of serpentinitic muds compared with the average composition of serpentinitic rocks (Table 3). The lack of admixtures of gabbroic material and sediment is indicated by low TiO_2, Y, and Zr concentrations.

2. *Serpentinitic mud with admixtures of slope sediment* (Sample 567-14-2, 131–133 cm). This type contains quartz and intermediate plagioclase and has distinct higher Al_2O_3 ,TiO_2 V, K_2O, Rb, Zr, and Ba concentrations (Table 3) than the first type. This second type contains expandable trioctahedral clay minerals.

3. *Serpentinitic mud with admixtures of gabbroic material* (Sample 567-20-1, 17–20 cm). A typical feature of this type is the admixture of detrital minerals of gabbroic origin. The chemical composition shows enrichment of all elements besides the ones that are typical of ultramafic rocks (MgO, Cr, Co, Fe_2O_3, and Ni, Table 3). Trioctahedral expandable clay minerals are strongly enriched in this type. K_2O and Ba show lower amounts than in the second type.

SUMMARY

The massive serpentinitic rocks that were mainly composed of the serpentine mineral lizardite were altered to chrysotile, which subsequently formed the serpentinitic muds drilled at Sites 566, 567, and 570. Expandable tri-

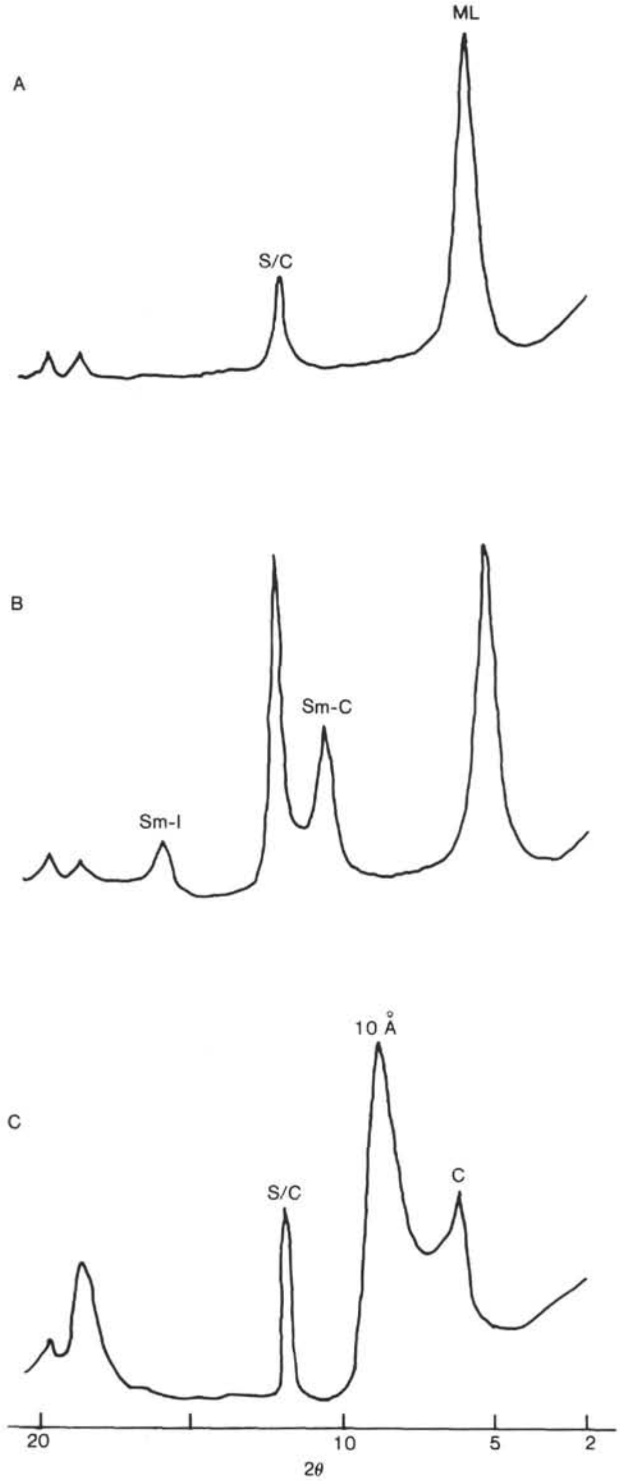

Figure 5. X-ray diffraction patterns (Cu, Kα) of swelling mixed layers, 567-17-1, 110–112 cm; (A) the untreated sample; (B) the glycolated sample; and (C) the sample after heating to 500°C. S, ML, Sm, C, and I refer to serpentine, mixed layer, smectite, chlorite, and illite, respectively. Sm-I and Sm-C refer to the (001) d-spacing of glycolated smectite–illite and smectite–chlorite mixed layer. 10 Å refers to the newly formed 10-Å structure of smectite after heat treatment. A weak Sm-I peak may be supposed under the Sm-C peak at 8.5 Å.

octahedral clay minerals are formed in the serpentinitic muds by alteration of chlorite and/or serpentine. The chemical composition of the serpentinitic muds reflects the amount of admixtures of slope sediment or gabbroic material.

ACKNOWLEDGMENTS

The author gratefully thanks Professor H. Füchtbauer for critically reading the manuscript and for his assistance with preparation of the English text. The author also acknowledges the critical reviews of Drs. M. Baltuck, W. C. Isphording, and W. B. Simmons. In addition, the author thanks S. Krosse for drafting the figures.

REFERENCES

Barnes, I., and O'Neil, J. R., 1969. The relationship between fluids in some fresh Alpine-type ultramafics and possible modern serpentinization. Western United States. *Bull. Geol. Soc. Am.*, 80: 1947–1960.

Boles, J. R., 1971. Synthesis of analcime from natural heulandite and clinoptilolite. *Am. Mineral.*, 56:1724–1734.

Brindley, G. W., and Brown, G., 1980. *Crystal Structures of Clay Minerals and Their X-ray Identification:* London (Mineralogical Society).

Coleman, R. G., 1977. Ophiolites. *Minerals and Rocks,* (Vol. 12): Berlin-Heidelberg-New York (Springer).

Faust, T. G., and Fahey, J. J., 1962. The serpentine-group minerals. *U.S.G.S. Prof. Paper,* 384-A:1–92.

Mackenzie, R. C., 1957. *The Differential Thermal Investigation of Clays:* London (Mineralogical Society).

Mumpton, F. A., and Thompson, C. S., 1975. Mineralogy and origin of the coalinga asbestos deposit. *Clays Clay Miner.,* 23:131–143.

Prichard, H. M., 1979. A petrographic study of the process of serpentinization in ophiolites and the ocean crust. *Contrib. Mineral. Petrol.,* 68:231–249.

Thorez, J., 1975. *Phyllosilicates and Clay Minerals. A Laboratory Handbook for Their X-ray Diffraction Analyses:* Dison, Belgique (G. Lelotte).

Yariv, S., and Heller-Kallai, L., 1975. The relationship between the I. R. spectra of serpentinites and their structures. *Clays Clay Miner.,* 23:145–152.

Date of Initial Receipt: 7 February 1984
Date of Acceptance: 7 March 1984

Table 3. Chemical composition of gabbros, serpentinites, average sediments, and serpentinitic muds.

	Average serpen-tinite	566-6-1, 10-12 cm		570-41-1, 78-80 cm		567-7-2, 77-79 cm		570-40,CC (7-9 cm)		567-17-1, 110-121 cm	567 Average sediment	567-14-2, 131-33 cm	567-14-2, 140-43 cm	567 Average gabbro	567-20-1, 17-20 cm	567-28-1, 80-82 cm
		(>63 μm)	(<63 μm)	(>63 μm)	(<63 μm)	(>63 μm)	(<63 μm)	(>63 μm)	(<63 μm)	(<63 μm)		(<63 μm)	(<63 μm)		(<2 μm)	(<63 μm)
Major and minor elements (wt.%)																
SiO_2	43.1	43.3	43.12	44.31	46.11	36.53	48.39	45.05	44.17	46.59	65.7	54.2	44.74	51.4	45.18	44.52
TiO_2	0.01	0.01	0.01	0.02	0.01	0.04	0.02	0.02	0.02	0.01	0.8	0.93	0.65	0.9	0.64	0.06
Al_2O_3	0.9	0.79	0.60	0.87	0.71	1.33	0.78	0.57	0.66	0.39	19.0	17.34	15.64	16.0	15.51	5.02
Fe_2O_3	8.3	9.32	8.18	8.75	7.78	10.66	5.73	10.85	9.09	6.59	6.6	9.88	17.55	11.6	17.41	7.21
MnO	0.1	0.12	0.09	0.09	0.10	0.29	0.05	0.08	0.1	0.09	0.1	0.18	0.32	0.2	0.32	0.11
MgO	45.73	42.12	43.2	43.13	44.10	34.84	43.69	38.02	40.88	44.96	2.6	12.65	15.94	9.3	15.81	41.99
CaO	0.5	2.22	0.97	2.4	0.74	15.49	0.58	5.73	3.79	0.03	1.4	1.03	2.91	8.1	2.89	0.49
Na_2O	0.01	0.22	1.59	0.01	0.01	0.01	0.01	0.01	0.01	0.03	1.5	1.39	1.42	2.05	1.41	0.01
K_2O	0.01	0.01	0.07	0.02	0.01	0.07	0.02	0.01	0.01	0.09	1.9	2.45	0.46	0.23	0.45	0.01
P_2O_5	0.01	0.07	0.07	0.01	0.01	0.04	0.02	0.02	0.02	0.01	0.2	0.16	0.07	0.08	0.07	0.01
S	0.1	0.02	0.52	0.04	0.02	0.18	0.18	0.02	0.02	0.39	0.1	0.18	0.02	0.1	0.02	0.11
Cl	0.01	0.01	0.02	0.01	0.01	0.01	0.01	0.01	0.01	0.01	0.01	0.01	0.01	0.01	0.01	0.01
Trace elements (ppm)																
V	36	41	21	49	39	37	25	39	28	31	128	185	345	211	342	44
Cr	2560	5546	2551	1389	1584	2941	1733	2043	1535	3076	83	124	233	221	229	2171
Co	65	50	50	36	27	49	54	56	43	68	16	27	56	39	60	48
Ba	1	1	6	1	4	214	47	1	13	0	751	719	177	62	176	1
Ni	3170	2151	2229	1318	1791	1590	2722	1741	1510	4528	66	84	225	187	224	2001
Cu	53	12	869	48	149	105	91	21	133	60	138	242	136	61	135	71
Zn	61	56	119	33	143	80	232	32	95	48	260	150	90	90	950	93
Rb	8	5	12	8	10	11	8	7	7	7	72	44	33	9	13	7
Sr	10	358	260	9	9	219	23	8	9	7	416	193	120	171	58	12
Y	1	1	1	2	1	1	1	1	1	0	28	24	16	16	16	1
Zr	10	11	12	13	13	18	14	14	15	9	161	110	82	53	35	12
Nb	2	1	1	4	10	1	1	1	2	1	6	1	3	6	1	1

Note: Iron is documented as total Fe_2O_3. The analyses have been calculated to a water-free basis (average sediment was calculated on a water- and carbonate-free basis). Average composition of 567 sediment and gabbro refers to samples of Site 567. Average composition of serpentinite refers to composition of all serpentinites of Sites 566, 567, and 570 investigated.

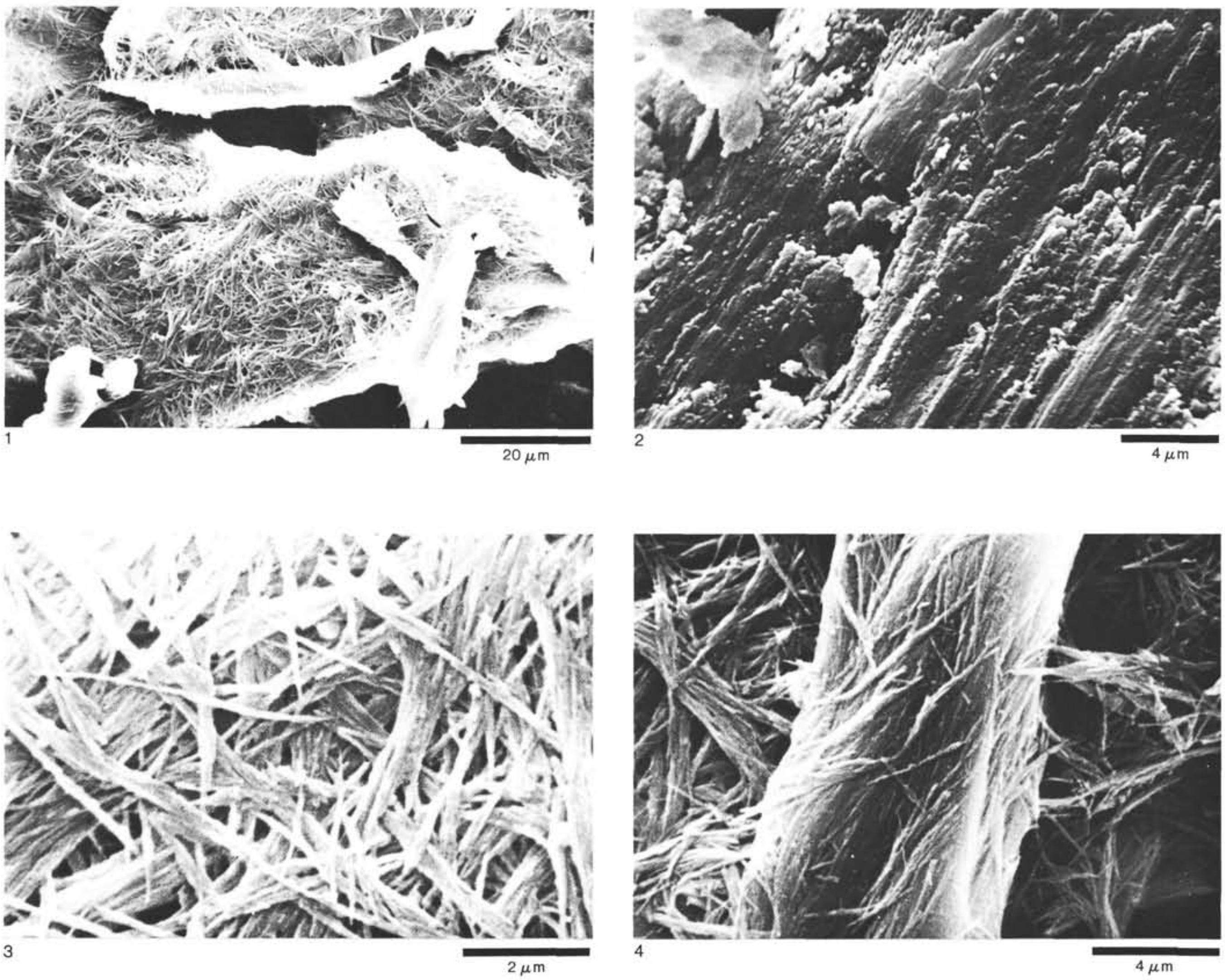

Plate 1. **1.** Electron photomicrograph showing chrysotile aggregates of serpentinitic mud. (570-39,CC [5–10 cm]). **2.** Electron photomicrograph showing oblique section of lizardite plates in massive serpentinites (570-41,CC [10–13 cm]). **3.** Electron photomicrograph showing chrysotile fibers at high magnification (570-39,CC [5–10 cm]). **4.** Electron photomicrograph showing bundles of chrysotile. Note shape of chrysotile fibers next to the aggregate (570-40,CC [7–9 cm]).

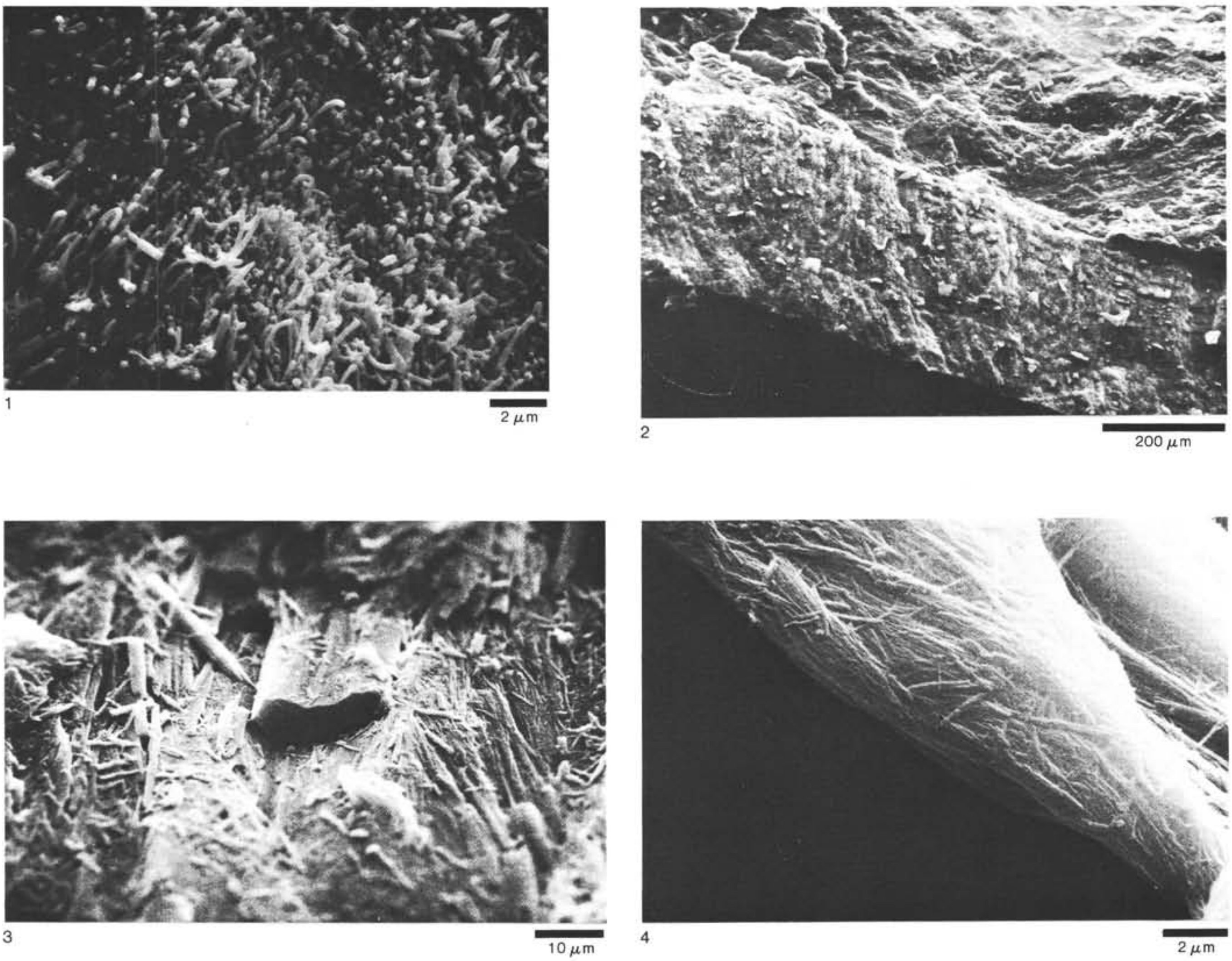

Plate 2. **1.** Electron photomicrograph showing chrysotile tubes in a vein of massive serpentinite. Note the difference in habit of chrysotile as compared to the chrysotile in serpentinitic mud (570-41-3, 65–68 cm). **2.** Chrysotile vein in serpentinite. Note the platy morphology of lizardite compared to the fibrous morphology of chrysotile in this sample (570-41-3, 65–68 cm). **3.** Electron photomicrograph showing tremolite crystals in a gabbroidic clast (567-21,CC [4–6 cm]); tremolite was identified using an EDAX system. **4.** Electron photomicrograph showing bundles of serpentine fibers indicating that chrysotile was formed from lizardite plates (570-41-1, 31–33 cm).